ELSEVIER

Journal of Photochemistry and Photobiology A: Chemistry 96 (1996) 79–92

Journal of PHOTOCHEMISTRY AND PHOTOBIOLOGY A:CHEMISTRY

Role of orbital overlap and local dynamics in long-distance electron transfer in photosynthetic reaction centres and model systems

Gertz I. Likhtenshtein

Department of Chemistry, Ben-Gurion University of the Negev, P.O.B. 653, Beer Sheva 84105, Israel

Received 3 August 1995; accepted 9 January 1996

Abstract

The following approaches have been developed to estimate the factors affecting electron transfer (ET) in proteins: (1) an analysis of the correlation between the rate constants of ET (k_{ET}) in a donor–acceptor (DA) pair and the dynamic parameters of various modes of relaxation of media traced by spin, fluorescent, triplet and Mössbauer labelling methods; (2) the use of spin exchange (SE) data in biradicals and complexes of transition metals with paramagnetic ligands and triplet–triplet energy transfer (TTET) data, which are considered as simple models of ET, for the estimation of the attenuation parameter (γ_X) of superexchange through an individual chemical group X and through homogeneous "conducting" and "non-conducting" media. The application of the aforementioned approaches to ET in photosynthetic reaction centres (RCs) and DA pairs in simple liquids and proteins is reviewed. The mechanism of ET in the systems under consideration is discussed. A new procedure of analysis of kinetic–thermodynamic relationships, including predictions by Marcus theory, is proposed.

Keywords: Long-distance electron transfer; Donor–acceptor pairs; Spin exchange; Triplet–triplet energy transfer; Photosynthetic reaction centres; Molecular dynamics; Proteins and membranes; Marcus theory

1. Introduction

Long-distance electron transfer (LDET) in proteins has been investigated extensively during recent decades [1]. Recent reviews are given in Refs. [1b–1g,1j,2]. The wide methodological and theoretical arsenal of chemical physics has been used to study LDET in proteins. In spite of the essential progress that has been achieved in measuring the LDET rate constants and in the theoretical treatment of the phenomenon, little is known about the factors which affect ET in proteins. The specific organization of a protein globule means that special properties are observed, such as a mosaic of local dynamics, a polarity effect and the capacity to delocalize electrons. From a review of the literature, it can be seen that the principal shortcoming in many recent approaches has been the underestimation of these special properties of proteins.

Some attempts, both theoretical and experimental, have been made to take into account the specificity of the electron pathways and local dynamics in proteins. This was performed by studying native and model systems with a known structure, e.g. donor–acceptor (DA) sites in photosynthetic reaction centres (RCs) and hybrid molecules consisting of a photoactive luminescent chromophore in the excited state as an electron donor and quinone or nitroxide radical as an acceptor [1e,1f,1j,1k,2a–2c,2e,2f,2i,3].

In an attempt to estimate quantitatively the factors which affect ET in proteins, the following approaches have been developed [3,4]: (1) an analysis of the correlation between the rate constants of LDET and various modes of intramolecular dynamics of the surrounding protein matrix traced by spin, fluorescent, triplet and Mössbauer labelling methods; (2) the use of spin exchange (SE) and triplet–triplet energy transfer (TTET) data in compounds with a known structure for the estimation of the attenuation parameter (γ) of superexchange through an individual chemical group including the peptide unit.

According to the theoretical treatment of outer-sphere ET, the effect of the dielectric relaxation of the medium on the ET dynamics depends on whether or not the solvent polarization is in equilibrium with the momentary electric charge distribution [1f,2i,2j,5]. The Marcus treatment of the adiabatic ET and non-adiabatic ET theory of Levich and Dogonadze implied that dielectric relaxation does not constitute the rate-limiting step [1j,6]. In the case of fast ET, the overall rate can be determined by the rate of the medium dipole reorganization [5a,5b]. Another situation occurs with the formation of conformationally or solvationally non-equilibrium redox states which react before the corresponding

PII S1010-6030(96)04305-5

equilibrium is established [2j,3b–3f,5k,5m,7]. Such processes may be detected in the analysis of the correlation between the rates of definite steps of ET and the molecular dynamics parameters of the medium. The latter can be monitored in proteins by the use of spin, fluorescent, triplet and Mössbauer labelling methods. Investigations in this direction were started in the late 1960s [8] and have revealed a general picture of protein intermolecular dynamics over a wide range of temperature and correlation time (τ_c) [3a,4a,4e,9].

As repeatedly stressed in the literature [3a,4a,10], there is a strong analogy between ET and SE interaction between paramagnetic centres. In both cases, the efficiency of the process is proportional to the value of the overlap integral S^n. As shown in Refs. [10] and [11], the value of the exchange integral ($J \sim S^2$) depends on the character of the bridge connecting the interacting centres. An examination of the experimental data on the exchange integral for SE between paramagnetic centres in biradicals and in metallo-complexes with paramagnetic ligands allows the attenuation of the exchange interaction between a nitroxide radical R and a paramagnetic group P (nitroxide, transition metal ion) in the structure RY–X–ZP (where X is a fragment of the bridge), compared with the interaction in the structure RY–ZP, to be quantified. The values of the attenuation parameters for various X groups can be tabulated and can be used for the analysis of alternative pathways of ET in protein and model systems.

The photosynthetic RCs of purple bacteria and photosystem I (PSI) of green plants and the DA pairs in model protein systems are convenient models for studying the factors affecting LDET in proteins. X-Ray structures of these photoenzymes with high atomic resolution are available [12]; the kinetic properties have been studied down to the subpicosecond time range, and the thermodynamics of the redox intermediates have been investigated [4,13]. The molecular dynamics properties of the RCs of photosynthetic bacteria and protein model systems have been investigated over a wide range of temperature and correlation time [3a,4].

In this paper, we review the experimental results and theoretical considerations on orbital overlap effects, the correlation between the rate constants of the elementary steps of LDET in RCs from native and model photoactive systems and the parameters of the local dynamics of the medium as measured by physical labelling techniques in the temperature range 77–300 K and at correlation times of milliseconds to subnanoseconds.

2. SE and TTET as models for LDET

2.1. General background

The general expression for TTET between donor (D) and acceptor (A) centres includes the exchange integral J_{TT} and the Franck–Condon factor FC [14]

$$k_{TT} = (2\pi/h)J_{TT}FC \quad (1)$$

The hamiltonian of the exchange interaction H_{ex} between spins with operators S_1 and S_2 is described by the formula [10b]

$$H_{ex} = -2J_{SE}S_1S_2 \quad (2)$$

In both of these cases, the value of the exchange integral is quantitatively characterized by the degree of overlap of the electron orbitals with unpaired electrons. In the first approximation

$$J \sim \prod_{ij} S_{ij} \quad (3)$$

where S_{ij} is the overlap integral of the ith and jth orbitals participating in the exchange. According to theory [10b]

$$S_{ij} \sim \exp(-\beta_{ij}R_{ij}) \quad (4)$$

where R_{ij} is the distance between the interacting centres and β_{ij} is a coefficient. Consequently

$$J \sim \exp(-\sum_{ij}\beta_{ij}R_{ij}) \quad (5)$$

If the values of β_{ij} and R_{ij} are approximately equal for all n interacting orbital pairs

$$J \sim \exp(-n\beta R) \quad (6)$$

It can be expected that, in the first approximation, $n = 2$ for SE involving two unpaired electrons and $n = 4$ for a process of TTET in which four orbitals are involved: orbitals of the donor in the excited state, the acceptor in the ground state, the donor in the ground state and the acceptor in the excited state.

The outer-sphere and intermolecular LDET between D and A centres is treated by the Fermi golden rule [1,3a,3b,15]

$$k_{ET} = (2\pi/h)|V|^2FC \quad (7)$$

where V is the resonance integral and FC is the Franck–Condon factor for a given ET. The resonance integral V is related to the overlap integral for wavefunctions of the initial (i) and final (f) states

$$V \sim S_{if} \sim \exp(-\alpha_{if}R_{DA}) \quad (8)$$

where R_{DA} is the distance between the donor and acceptor centres and α is a decay coefficient.

Eqs. (7) and (8) are analogous to Eqs. (1)–(6), and thus the exchange phenomenon may be considered as an idealized model of ET. Therefore the determination of the dependence of the exchange parameters k_{TT} and J on the distance between the exchangeable centres and on the chemical nature of the bridge between the centres will be extremely fruitful for evaluating such dependences for the resonance integral in the ET formulae.

2.2. Static exchange: dependence on the distance and media

A vast literature is concerned with the quantitative investigation of exchange processes (see, for example, Refs. 3a,4a,10]). The quantitative exchange parameters, the rate constant of TTET (k_{TT}) and the exchange integral of the spin–spin interaction (J_{SE}) depend on the distance (R) between the exchangeable centres. The experimental data lie on two curves (Fig. 1) which are approximated by the following equation [3a,4a,10a,10h–10k]

$$k_{TT},\ J_{SE} = 10^{16} \exp(-\beta R) \quad (9)$$

For systems in which the centres are separated by a "non-conducting" medium (molecules or groups with saturated chemical bonds), $\beta_{TT} = 2.6$ Å^{-1}. For systems in which the radical centres are linked by "conducting" conjugated bonds, $\beta_{SE} = 0.3$ Å^{-1}.

We can consider the ratios

$$\gamma_{TT(R)} = k_{oTT}/k_{TT}(R);\ \gamma_{SE(R)} = J_{oSE}/J_{SE}(R) \quad (10)$$

(where k_{oTT}, J_{oSE} and $k_{TT}(R)$, $J_{SE}(R)$ are the values of the TTET rate constants and exchange integrals at the van der Waals' exchange distance and the distance R respectively) as a parameter of attenuation of the exchange interaction of TTET through a given medium. Taking into account Eq. (6), with the values $n = 4$ for TTET and $n = 2$ for SE and ET, and Eqs. (10), we have an expression for the dependence of the attenuation parameters of SE and ET (γ_{SE} and γ_{ET} respectively) on the distance R_{DA}

$$\gamma_{ET} = \gamma_{SE} = \exp(\beta_{DA} R_{DA}) \quad (11)$$

with $\beta_{DA} = 0.5\beta_{TT} = 1.3$ Å^{-1} for a "non-conducting" medium and $\beta_{DA} = \beta_{SE} = 0.3$ Å^{-1} for a "conducting" bridge. The value of β_{DA} for the "non-conducting" medium is close to that obtained by analysis of the experimental dependence of k_{ET} on the distance R_{DA} in model systems [10k,13h].

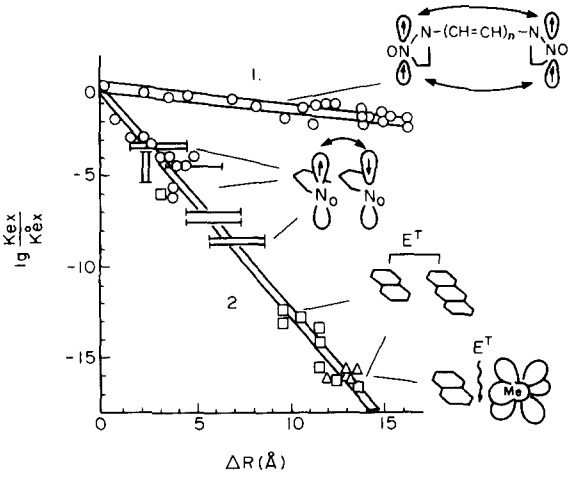

Fig. 1. Dependence of the logarithm of the relative parameters of the exchange interaction on the distance between the interacting centres (R); $k_{ex} = J_1 k_{TT}$; J is the exchange integral of interaction between paramagnetic centres; k_{TT} is the rate constant for triplet–triplet energy transfer (denoted as E^T; 1 and 2 are conducting and non-conducting media respectively) [3a,4a,10a,10k].

2.3. SE through individual groups

An examination of the empirical data on the exchange integral values (J) for the spin–spin interaction in systems with a known structure, e.g. biradicals, transition metal complexes with paramagnetic ligands and monocrystals of nitroxide radicals, allows the value of the attenuation parameter γ_X for exchange interaction through a given group X to be estimated. By our definition, the γ_X value is

$$\gamma_X = J_{RYZP}/J_{RYXZP} \quad (12)$$

where R is a nitroxide or organic radical, P is a paramagnetic complex or radical and X, Y and Z are chemical groups in the bridge between R and P.

Table 1 shows the results of the calculation of the attenuation parameter γ_X by Eq. (12). As can be seen from Table 1, the values of γ_X for X ≡ C=O, S=O, P=O, C_6H_4 and C=C, calculated from independent experimental data, are similar. The value $\gamma_C = \gamma_{C=O}$ was taken for further consideration because the O atom does not influence markedly the value of γ (Table 1).

Supposing that the value of the overall attenuation parameter for the exchange interaction along a chain of chemical groups is governed by

$$\gamma_{ov} = \prod_i^i \gamma_i \quad (13)$$

with i being an index of the intervening group, we can estimate the unknown value of γ_j using the equation

$$J_y = J_{oo}\gamma_j\alpha_1\alpha_2\prod_i^i \gamma_i^{-1} \quad (14)$$

where J_y is the exchange integral for a given biradical or paramagnetic complex, α_1 and α_2 are the spin densities on the radical fragments, $J_{oo} = 10^{16}$ s^{-1} is the pre-exponential factor of empirical Eq. (9) and γ_i are the known γ values for atoms of compound y. The empirical value of J_{oo} is obtained as J extrapolated to zero distance between exchangeable centres. The value of the attenuation parameter for the oxygen atom γ_O was estimated by the following procedure. We can represent the exchange integral $J_1 = 10^8$ s^{-1} for a biradical [11b,11f]

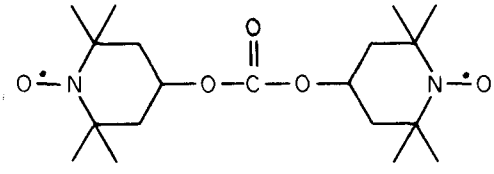

as a product

$$J_1 = 10^{16}\alpha^2 m^2(\gamma_{C=O})^{-1}(\gamma_C{}^{-2})(\gamma_C{}^{-4})(\gamma_O{}^{-2}) \quad (15)$$

where $\alpha = 0.5$ is the relative spin density on the nitrogen atom in the biradical nitroxide fragment [11a], $\gamma_C = \gamma_{C=O} = 8.4$ (Table 1) and $m = 2$ is a coefficient due to the involvement

Table 1
Values of the attenuation parameter of individual groups (γ_X), van der Waals' contact (γ_v) and hydrogen bond (γ_{hb}) for spin exchange processes in biradicals (RY–X–ZR) and paramagnetic complexes of transition metals with nitroxide ligands (RY–X–ZM). Values of the attenuation parameter γ_X for individual chemical groups were calculated using the formula $\gamma_X = J_{RYZM}/J_{RYXZM}$, where J_i are the experimental values of the exchange integral taken from the corresponding references (see Section 2.3)

Group, X	γ_X	Reference	Group, X	γ_X	Reference
C_6H_4	6±0.03	[10g,11a,11c,16]			
C=C	1.7	[10g,17]	H O | || –N–C–	55 [b]	
C=O C	8.4±0.4	[10d,10g, 11c–11g]	γ_v γ_{hb}	50 [a] 10 [a]	
			H	12 [a]	
NH	6.5	[10g,11d]	SO_2	2.2	[10g,11d]
O	5 [a]		RP=O	2.4±0.03 [c]	[10g,11d]
S=O	2.1	[10g,11d]			
	3.5	[10g,17]			

[a] Calculated in Section 2.3.
[b] Calculated by equation $\gamma_X = \gamma_{CO}\gamma_{NH}$.
[c] R ≡ Ph–, CH_2=CH–, Ph–CH=CH–, Ph–CCl=CH.

of two superexchange pathways in each of the two nitroxide radical fragments. According to Eq. (15), $\gamma_O = 5$.

The value of the attenuation parameter for the exchange interaction through van der Waals' contacts, $\gamma_v = 50$, was derived from Ref. [10b]. This value was calculated by the method of Owen [18]. The attenuation parameter for the hydrogen bond was estimated by comparing experimental data on the exchange integral J for two structures [10b,19]

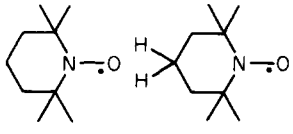

$J = 1.6 * 10^{11}\ s^{-1}$

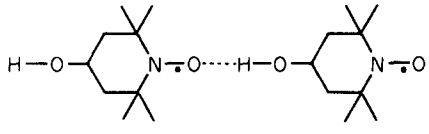

$J = 1.6 * 10^{11}\ s^{-1}$

In the first structure, the pathway of superexchange involves a van der Waals' bond and the hydrogen atom; in the second structure, SE occurs through the hydrogen bond, hydrogen and oxygen atoms. Considering Eq. (13), with the values $\gamma_v = 50$ and $\gamma_O = 5$ (Table 1), we have

$$\gamma_O\gamma_H\gamma_{hb}(H....O) = \gamma_H\gamma_v \quad (16)$$

and the value of the attenuation parameter for the hydrogen bond $\gamma_{hb} = 10$.

The attenuation of the exchange process passing through an H atom was estimated using Eq. (14) on the basis of the experimental data on the exchange integral J_y for the structure [10b,20]

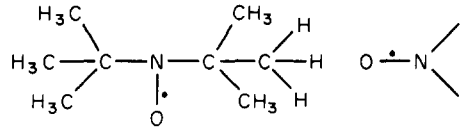

$Jy = 6 * 10^{10}\ s^{-1}$

According to Eq. (14)

$$J_y = 10^{16}\alpha_1\alpha_2(\gamma_C^{-2})(\gamma_H^{-1})(\gamma_v^{-1})$$

and the calculated value of $\gamma_H = 12$.

The data on the attenuation parameter presented in Table 1 can be used to analyse the effects of orbital overlap in ET in biological and model systems with known structures. From Eqs. (7)–(11), we can write the expression for the resonance integral

$$V = V_0\gamma_{DA}^{-1/2} \quad (17)$$

where V_0 is the value of the resonance integral at the van der Waals' distance; we can calculate the rate constant of non-adiabatic LDET using the following formula

$$k_{ET} = (2\pi/h)|V_0|^2\gamma_{ET}^{-1}FC$$
$$= (2\pi/h)|V_c|^2\exp(-\beta_{DA}R_{DA})FC \quad (18)$$

which is valid in the case of non-specific, "non-conducting" homogeneous media. For LDET along a specific pathway through a chain of covalent, hydrogen and van der Waals' bonds, we can use the formula

$$k_{ET} = (2\pi/h)|V|^2\gamma_{DA}^{-1}FC \quad (19)$$

where γ_{DA} is the product of all the attenuation parameters of the individual chemical groups γ_i, hydrogen bonds γ_{hb} and van der Waals' contacts γ_v

$$\gamma_{DA} = \prod_{i} \gamma_v \gamma_i \gamma_{hb} \quad (20)$$

Eqs. (17)–(20) are used in the next section to analyse the orbital overlap effects in ET in photosynthetic RCs and model systems.

3. Physical labelling methods to study the intermolecular dynamics and local polarity of proteins

The principle of physical labelling involves the modification of chosen sites of the object of interest by special compounds (labels and probes) whose properties make it possible to trace the state of the biological matrix by appropriate physical methods. Three main types of compound are used as labels and probes to monitor the dynamic properties of the system of interest: (1) centres with unpaired electrons and spins (stable nitroxide radicals and paramagnetic metal complexes); (2) luminescent, fluorescent and phosphorescent chromophores; (3) Mössbauer atoms (e.g. ^{57}Fe) which yield the nuclear γ-resonance (NGR) spectra.

3.1. Spin labelling

Data on the mobility of the nitroxide fragment of labels or probes in model systems at a correlation time $\tau_c = 10^{-4}$–10^{-11} s may be summarized as follows [3a,4a,8f,21]. In liquids, the mobility parameters of the fragment, including the activation parameters, are close to those of the molecules of the medium. In polymers, at temperatures higher than the glass transition temperature T_g, the mobility of spin probes is mainly determined by the segmental mobility of the polymeric chains. Below T_g, the mobility of the probes is modulated by relatively low amplitude motions of the matrix walls which surround the probe.

The magnetic parameters of nitroxide radicals, the g factor and the hyperfine splittings A_{iso} and A_{aniso} are sensitive to the properties of the medium, e.g. the micropolarity and ability to form H bonds with the N–O$^{\cdot}$ group. For example, $A_{iso} = 1.4 + 0.064(\epsilon_0 - 1)/(\epsilon_0 + 1)$, where ϵ_0 is the dielectric constant and A_{iso} is given in mT.

3.2. Fluorescent labels

The excitation of a chromophore is accompanied by a change in the electric dipole moment of the molecule. This involves a change in the energy of interaction with the surrounding dipolar molecules. If the characteristic time of reorganization relaxation of the dipoles (τ_r) in the medium is much longer than the lifetime of fluorescence or phosphorescence τ^*, the dipoles have no chance to follow the change in the light-induced electric field, and a transition from the "unsolvated" excited state to the ground state takes place. In another limiting case, where $\tau_r \ll \tau^*$, the interaction between the dipoles and the excited molecule lowers the energy of the system, and the emission is from the "solvated" level. The relaxation can be followed by time-resolved spectroscopy, measuring the kinetics of the shift of the maximum of the fluorescence or phosphorescence spectrum $\nu_{max}(t)$ (relaxation shift) [3a,4a,22]

$$[\nu_{max}(t) - \nu_{max}(\infty)]/[\nu_{max}(0) - \nu_{max}(\infty)] = \exp(-t/\tau_r) = P \quad (21)$$

where the indices t, "∞" and "o" are related to ν_{max} of the time-resolved emission spectrum at a given moment t, $t \to \infty$ and $t = 0$. The value of τ_r can also be estimated by measurement of the temperature dependence of $\nu'_{max}(T)$ of the steady state emission spectrum using the formula

$$[\nu'_{max}(T) - \nu'_{max}(\infty)]/[\nu'_{max}(0) - \nu'_{max}(\infty)] = \tau^*/(\tau^* + \tau_r) = P' \quad (22)$$

The values P and P' can be considered as empirical parameters of the relative time-dependent (dynamic) polarity.

However, in real systems, deviations from the abovementioned simple physical picture are observed, caused by the effect of the electric field of the excited chromophore on the motion of the medium molecules in the vicinity of the chromophore (induced relaxation) and by the intrinsic microheterogeneity of the samples. If we assume a gaussian distribution of the free activation energies (ΔF) of the orientation of the chromophores, it is possible to find an expression for the apparent activation energy [3a,4a,23]

$$E_{app} = E_{max} - \Delta F_o^2/RT$$

where E_{max} is the most probable activation energy and ΔF_o^2 is the second moment of the distribution curve. The values of E_{max} were found to be close to the activation energy of dielectric relaxation in the bulk solvent. The distribution parameters ΔF_o, obtained by analysis of the temperature-dependent relaxation shift of the phosphorescence spectra in simple liquids, were similar to that established using the time-resolved technique [23].

As shown in Ref. [24], at high temperature, the Arrhenius plot $\tau_r(T)$ calculated using Eq. (21) is related to the spontaneous dielectric relaxation in the bulk solvent. At low temperature, the induced relaxation appears to be the main contribution to P'. Extrapolation of the high temperature Arrhenius plot $\tau_r(T)$ to low temperature allows the parameters τ_r and P'_v to be calculated. The latter is related to the effective dynamic polarity in the bulk solvent at all available temperatures.

Correlation can be expected between the kinetic parameters of ET and P'_v for processes limited by the spontaneous motion of the medium molecules. If ET is controlled by induced relaxation, a correlation may exist between the kinetics and the local dynamic parameter P'.

3.3. Mössbauer labels

The integrated intensity of Mössbauer (NGR) spectra (f') is related to the amplitude of the mean displacement of the

^{57}Fe nucleus in the recoil direction ($\langle x^2 \rangle$) during the lifetime of the excited state ($\tau_n^* = 1.4 \times 10^{-7}$ s) [3a,4a–4d,8d]

$$f' = \exp(-4\pi^2 \langle x^2 \rangle / \lambda^2) \quad (23)$$

where λ is the γ-quantum wavelength and x is in nanometres. If the ^{57}Fe nucleus participates in Brownian motion with a diffusion coefficient D and the Stokes–Einstein law is fulfilled, the magnitude of the relative broadening of the spectrum is given by

$$\Delta\Gamma/\Gamma = 10T/\eta R \quad (24)$$

where η (P) is the viscosity and R (nm) is the radius of the particle that is rigidly linked to the nucleus. The foregoing formulae represent the effect of the dynamics of the medium on the NGR spectrum. For example, when the amplitude of the ^{57}Fe vibration increases by 0.05 nm, f' decreases by a factor of 10^5. Such properties can be used to study the dynamics of biological objects.

4. LDET in RCs: orbital overlap effects

The following scheme of ET in the RC of photosynthetic bacteria has been shown to take place [1e,12,13]

$$\underset{P}{(Bchl)_2} \text{ —— } Bchl \longrightarrow \underset{H}{Bph} \longrightarrow Q_A \longrightarrow Q_B$$

where the bacteriochlorophyll dimer $(Bchl)_2$ (P) is the primary donor, Bchl is bacteriochlorophyll, Bph (H) is bacteriopheophytin and Q_A and Q_B are the primary and secondary quinone acceptors respectively.

In the RC of PSI, the primary photochemical steps occur along the cascade of the redox centres [1g,12c,13]

$$P700 \longrightarrow A_0 \longrightarrow A_1 \longrightarrow F_X \longrightarrow F_A$$

where P700 is the chlorophyll dimer, A_0 is chlorophyll, A_1 is phylloquinone and F_X and F_A are the 4Fe–4S clusters.

Experimental rate constants of ET (k_{ET}) in RCs of purple bacteria and PSI are plotted against the edge–edge distance (R) between the donor and acceptor centres in Fig. 2. The dependence of log k_{ET} on R is similar to that found for biological and model systems reported elsewhere [13h]. It should be stressed that the slope of the curve corresponds to the slope of log γ_{ET} vs. R_{DA}, predicted for long distance superexchange orbital overlap through "non-conducting" media by the shortest pathway (Eqs. (11) and (18) with $\beta_{DA} = 1.3$ Å^{-1}).

For the first step of ET from the primary donor (bacteriochlorophyll dimer, P) to the intermediate bacteriopheophytin acceptor (H) and from P700 to the pheophytin intermediate acceptor, the experimental rate constants are considerably larger than those expected from Eq. (18) and the "regular" dependence shown in Fig. 2. Such a deviation has been explained elsewere [1d,13a,13e,15g].

Another deviation is related to ET from the primary quinone acceptor Q_A to the secondary quinone acceptor Q_B. The

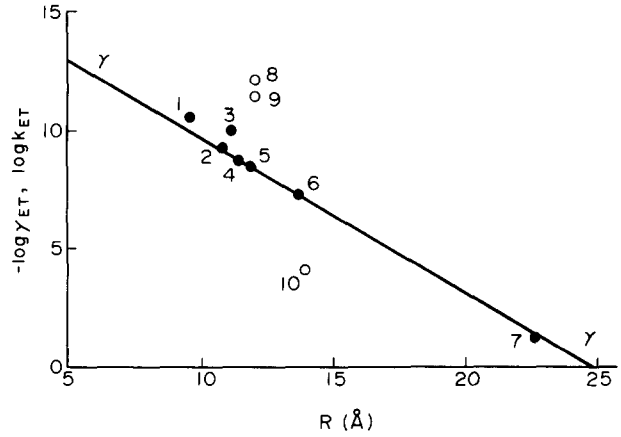

Fig. 2. Dependence of the experimental rate constants of ET (k_{ET}) in photosynthetic RCs of bacterial and plant PSI [1e,13] on the edge–edge distance between the donor and acceptor centres (R) [12]: 1, $A_0^- \rightarrow A_1$; 2, $H^- \rightarrow Q_A$; 3, $A_1 \rightarrow F_X$; 4, $H^- \rightarrow P^+$; 5, C559 $\rightarrow P^+$; 6, $F_X \rightarrow F_A$; 7, $Q_A^- \rightarrow P^+$; 8, $P^- \rightarrow$ Bchl; 9, P700 $\rightarrow$ Chl; 10, $Q_A^- \rightarrow Q_B$. The straight line is related to the dependence of the attenuation parameter $\gamma(R)$ derived from Eqs. (11) and (18) for SE and ET processes in homogeneous "non-conducting" media. Filled circles correspond to a "regular" dependence, open circles to a "deviation".

process takes place at an edge–edge distance of about 14 Å, but there is an intermediate with two hydrogen bonds and an Fe atom coordinated with two imidazole groups [1e,12a,12b,12d]. The estimation of the resonance integral V_{QAQB} for the process was based on this fragment of the X-ray model of RC using the values of the attenuation parameter γ_X (Table 1) and Eq. (15), which gives in this case

$$V_{QAQB} = V_{0hb}(\gamma_{im}^{-1})(\gamma_M^{-1/2})$$

where $\gamma_{im} = \gamma_X = 3.3$ (X is the thiophene group), γ_M is the γ value of the Fe atom with its highly conducting d orbitals ($\gamma_M^{-1/2} = 1$ndash;0.7) and V_{0hb} is the resonance integral for a hydrogen bond. The latter value is larger than that at the van der Waals' distance $V_0 = 2.5$ eV. As a consequence, $V_{QAQB} > 0.5$ eV and exceeds the limit for adiabatic processes ($V_{ad} = 2.5 \times 10^{-2}$ eV at room temperature). This implies that ET from the primary acceptor to the secondary acceptor runs adiabatically in spite of the relatively large distance between Q_A and Q_B.

A quantitative estimate of the resonance integral allows the coupling and Franck–Condon effects of ET in the photosynthetic RCs to be analysed separately (see Section 5).

5. Kinetics of ET and molecular dynamics in the RC of photosynthetic bacteria

Complex systems, such as globular proteins, undergo a number of dynamic processes, which have specific frequencies and amplitudes. A wide range of physicochemical methods have been used to study the intramolecular dynamics of protein globules and adjacent solvent and lipid molecules. The joint application of spin, fluorescence, triplet, Mössbauer and radical pair labelling techniques makes it possible, in

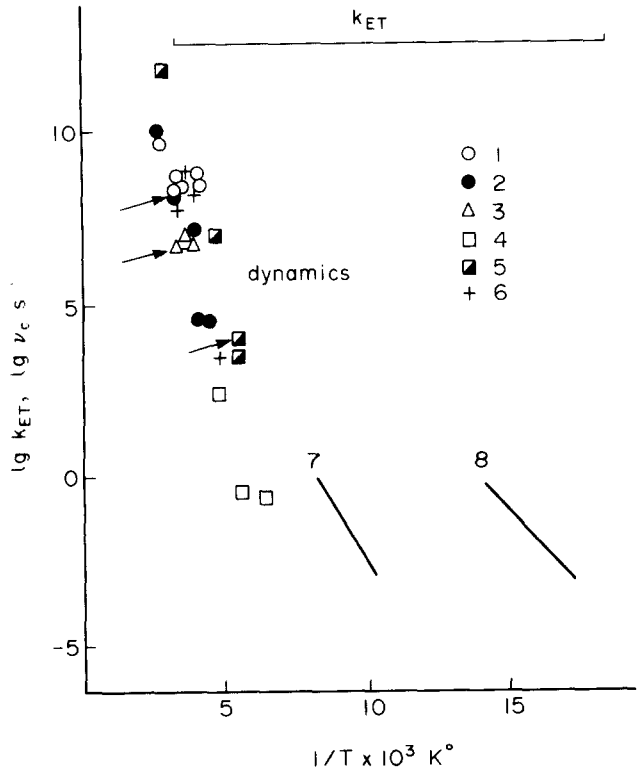

Fig. 3. Data on the correlation frequency of the mobility of physical labels and their environment in bovine and human serum albumins and in the RC of *R. sphaeroides* [3a,4], and rate constants of ET from the primary donor P to the bacteriopheophytin acceptor H (k_{PH}) [13c] in the Arrhenius coordinates. 1, fluorescent labels; 2, spin labels; 3, Mössbauer labels; 4, phosphorescent labels; 5, translational jumps of O_2; 6, PMR; 7, 8, Arrhenius dependence calculated from the experimental data on the recombination of radical pairs and diphenylamine radicals in hydrophobic centres for fractions with maximum (7) and minimum (8) activation energy of recombination; straight line is related to the experimental temperature dependence of k_{PH}. Arrows indicate the data related to the experimental parameters of the dynamics of the RC.

particular, to study the dynamics over an extensive range of characteristic correlation times $\tau_c = 10^{-2}$–10^{-10} s. Such studies have been pursued for a number of proteins including RCs of photosynthetic bacteria [3,4,8].

Fig. 3 shows the Arrhenius dependence of the correlation frequencies of the dynamic processes in bovine and human serum albumins. A general trend can be seen in Fig. 3: the lower the value of the characteristic frequency of the method applied, the lower the temperature at which the label mobility can be recorded. In the wide temperature range of 130–300 K, the experimental data for the labels located on the protein globule surface lie around an Arrhenius straight line with an activation energy $E_{app} = 70$ kJ mol^{-1} and an activation entropy $\Delta S_{app} = 160$ eu. Thus the mobility is the result of a gradual softening of the water–protein matrix rather than of individual phase transitions. The mobility of the hydrophobic spin probe and diphenylamine radical pair in the hydrophobic pocket of human serum albumin was characterized by the following parameters: $E_{app} = 20$ kJ mol^{-1} and $\Delta S_{app} = -23$ eu in the temperature range 50–280 K [3a,4a].

Physical labelling has been applied to the investigation of the molecular dynamics properties of RCs extracted from *R. sphaeroides* in the isolated state and incorporated into chromatophore membranes [3a,4]. This system appears to be an ideal model for the analysis of the possible correlation between dynamics and ET.

Spin, Mössbauer, fluorescent and phosphorescent labels were introduced into various portions of the photosynthetic membrane; they were covalently bound to the surface groups of the RC, adsorbed by the hydrophobic segments of proteins and the lipid portions of the membrane, and ^{57}Fe atoms were introduced by way of biosynthesis into iron-containing proteins. In these samples, the dependence of the label mobility and rate constant of ET between the components of the photosynthetic chain on the temperature and moisture content was measured. The results from some of the experiments are illustrated in Figs. 4 and 5. It can be seen from Fig. 4 that the emergence of an electron from the primary photosynthetic cell, i.e. transport from the primary acceptor Q_A to the secondary acceptor Q_B, takes place only under conditions in which the labels record the mobility of the protein moiety of the membrane with $\tau_c < 10^{-7}$ s. This time is at least 10^3- fold

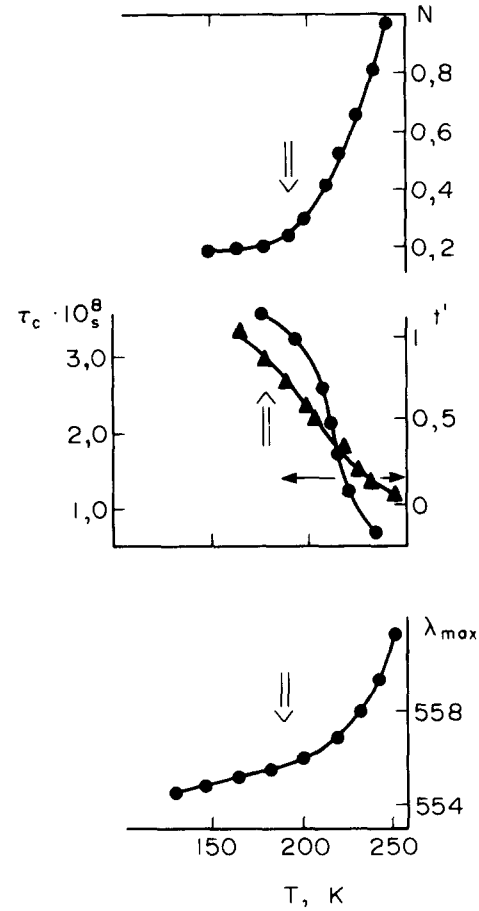

Fig. 4. Temperature dependence of the effectiveness of ET (N) from the primary acceptor (Q_A) to the secondary acceptor (Q_B), correlation time of spin label rotation (τ_c), intensity of the NGR spectrum (f') of the Mössbauer label (^{57}Fe) and maximum of the fluorescent label (fluorescein) emission spectrum (λ_{max}) in chromatophores from *R. rubrum* [3a,4a].

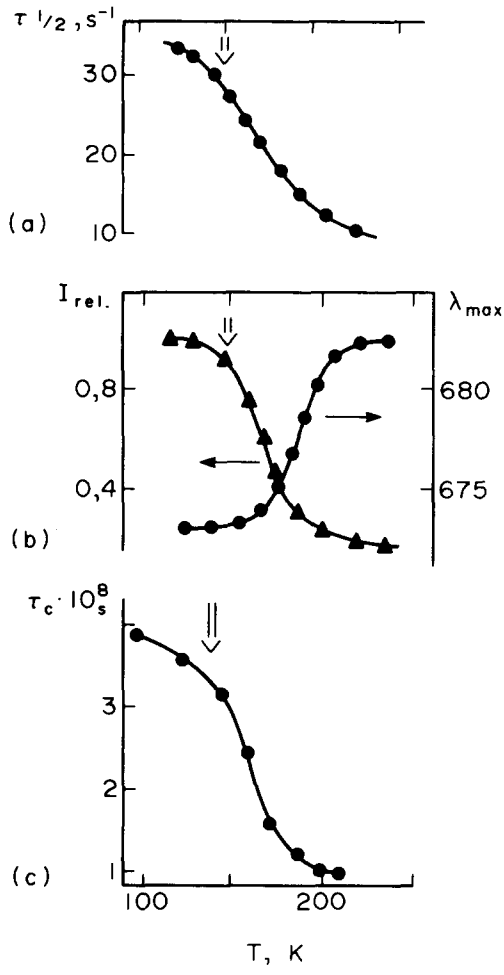

Fig. 5. Temperature dependence of the characteristic time of ET ($\tau_{1/2}$) from the reduced primary acceptor (Q_A^-) to the oxidized primary donor (P^+) (a), intensity (I_{rel}) and maximum wavelength (λ_{max}) of the phosphorescence spectrum of eosin attached covalently to membrane proteins (b) and τ_c of the spin label in the chromatophore membranes from *R. rubrum* (c) [3a,4a].

longer than the time of ET (k_{ET}). Therefore, in this case, thermal equilibrium between the donor–acceptor centres and the surrounding protein medium throughout the process can be assumed.

The rate constant of recombination between the reduced primary acceptor (Q_A^-) and the oxidized primary donor (P_1^+) decreases from 30 to 10 s^{-1} when dynamic processes with $\tau_c = 1–10^{-3}$ s occur (Fig. 5). This result may be caused by a slight change in the distance between and/or mutual orientation of the centres.

Fig. 3 shows that the values of the correlation frequency of mobility of spin, fluorescent, triplet and Mössbauer labels introduced into RCs agree reasonably well with the general Arrhenius plot. As shown in Fig. 3, a drastic change in the molecular dynamics parameters as a function of temperature is not accompanied by a significant change in the rate constant of ultrafast ET (k_{PH}) from the primary donor (P) to the intermediate acceptor bacteriopheophytin (H). Throughout the experimental temperature range, $k_{PH} = 3.3 \times 10^{10}$ to 4×10^{11} s^{-1}. For ET from H^- to Q_A, $k_{HQA} = 5 \times 10^9$ s^{-1} [1e,13a,13e], which is markedly larger than the correlation frequency $\nu_c = \tau_c^{-1} < 10^9$ s^{-1}. Therefore ET occurs more rapidly than orientational relaxation of the protein medium.

6. ET and local dynamics in donor–acceptor pairs (DAPs) in model protein and liquid systems

6.1. DAPs in liquids

In order to determine the influence of the molecular dynamics and local polarity of the medium on ET, the effect of the temperature and nature of the solvent on a model photochemical reaction, involving the reduction of a nitroxide radical covalently bound to a photoactive chromophore, was studied [3b–3f].

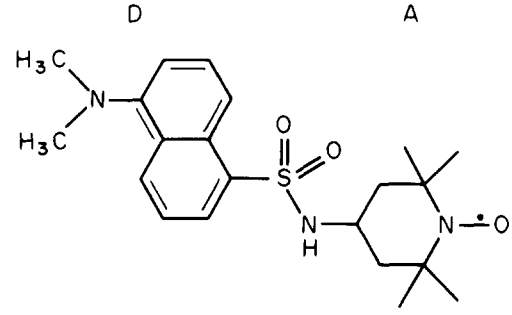

In such a hybrid molecule, the chromophore fragment in the excited state (D^S) can serve as an electron donor and the nitroxide fragment as an acceptor (A). The process of D^S quenching by the nitroxide fragment of the DAP can be monitored by time-resolved and steady state fluorescence techniques; the photoreduction of the nitroxide fragment, which is accompanied by enhanced fluorescence, can be followed by electron spin resonance (ESR) spectroscopy and, independently, by the fluorescence technique.

As shown in Refs. [3b] and [3c], the efficiency of intermolecular quenching, controlled by monitoring the steady state fluorescence intensity of DAP in solution (75% glycerol, 20% water and 5% ethanol), is not dependent on the

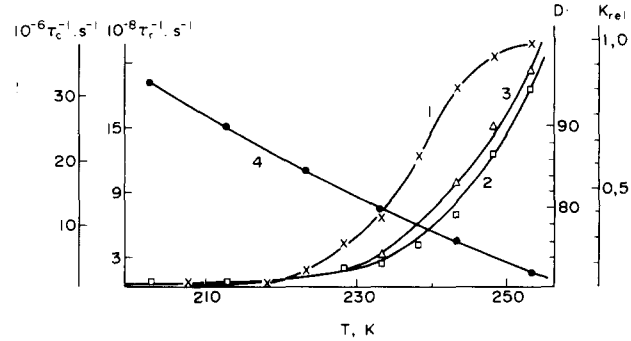

Fig. 6. Temperature dependence of: 1 the relative rate constant of photoreduction of the nitroxide fragment (k_{rel}); 2 solvent relaxation time in the vicinity of the excited chromophore fragment (τ_r); and 3 correlation time of the nitroxide rotation (τ_c) in DAP in solution (75% glycerol, 20% water and 5% ethanol) [3b], D is the dielectric constant of the solution.

temperature in the range 170–300 K in conditions which exclude the irreversible photoreduction of nitroxide (Fig. 6).

The process of quenching was studied by picosecond fluorescence single photon counting spectroscopy in glycerol and cyclohexane solutions [25]. The application of decay time distribution analysis to the fluorescence and relaxation shift kinetics shows that intermolecular fluorescence quenching of the donor occurs 2–10 times faster than solvent relaxation in the vicinity of the excited chromophore and non-radiative quenching (Table 2). The characteristic quenching time is found to be only slightly dependent on the temperature and on the momentary and static polarity of the medium. It should be noted that ET in DAP is thermodynamically favourable even in non-polar solvents and at low temperature (Fig. 7, see below).

Three mechanisms of quenching can be proposed [3b–3f,25,26]: (1) Forster resonance energy transfer; (2) exchange processes; (3) reversible ET. The first mechanism can be rejected because of the very weak overlap of the emission spectrum of the donor and the absorption spectrum of the nitroxide and the violation of the spin conservation rule. At present, it is difficult to discriminate between the second and third mechanisms of quenching. Nevertheless, some established criteria can be formulated.

As shown in Section 2.2, the dependence of the parameters of exchange processes on the distance is steeper than that for ET and SE (Fig. 1). For a distance $R=8$ Å between the nitroxide group of the acceptor and the donor edge in DAP, the value of k_{TT} is expected to be about $10^8\ s^{-1}$, i.e. markedly lower than the experimental value of $k_q=3\times10^{11}\ s^{-1}$. For such a distance, the maximum rate constant of ET, expected theoretically from the data on SE and the experimental data (Fig. 2), is $k_{ET}=10^{11}$–$10^{12}\ s^{-1}$. On the other hand, the latter value can be reduced by the Franck–Condon factor (Eq. (7)). Therefore a preference for exchange mechanisms at short distances over ET may be expected. The latter seems to be more favourable at long distances.

If the intensity of the incident light is sufficiently high, the photoreduction of the DAP nitroxide fragment to the corresponding hydroxylamine is accompanied by a parallel decrease in the nitroxide ESR signal and an increase in the fluorescence intensity [3b–3f,26c]. The temperature dependence of the relative rate constant of photoreduction k_{rel} correlates with that of the solvent relaxation in the vicinity of the excited chromophore, the relaxation shift of the DAP chromophore fragment (τ_r) and the ESR parameter of nitroxide mobility (τ_c) (Fig. 6). The analysis of the energy diagram

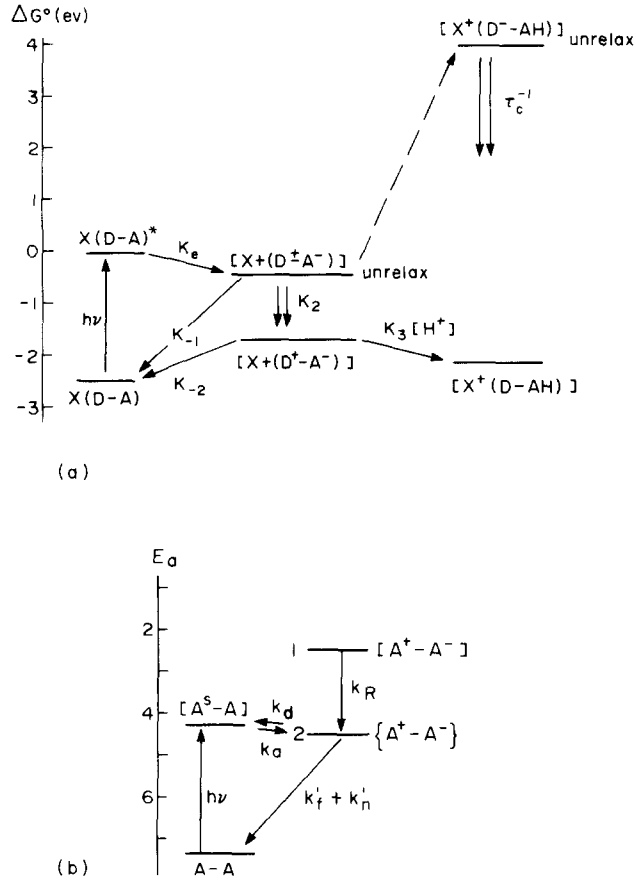

Fig. 7. Diagrams of the energy levels for ET in DAP in BSA molecules [3f] (a) and for ET in excited biantril [28] (b). 1 and 2 are unrelaxed and relaxed states respectively.

of the process (Fig. 7(a)) confirms that, in the given case, nanosecond relaxation of the medium is necessary to provide favourable energetics for the reduction of the nitroxide fragment.

6.2. Biantril in solutions

Another convenient model for the analysis of the relationship between ET and the solvent dynamics is biantril, which consists of two identical moieties of antril (A–A), electronically independent for steric reasons [27,28]. The energy diagram of photo-ET with the formation of the ion pair A^+–A^- is shown in Fig. 7(b). In the steady state condition, the apparent equilibrium constant

Table 2
Parameters of intermolecular fluorescence quenching ($\tau_q=k_q^{-1}$), relaxation of the solvent (τ_{r1}, τ_{r2}), momentary dielectric constant ϵ_m and macroscopic viscosity (η) in the hybrid molecule DAP with dansyl chromophore as donor and nitroxide fragment as acceptor [25]

Solvent	T (°C)	τ_q (ns)	τ_{r1} (ns)	τ_{r2} (ns)	ϵ_m	η (cP)
Cyclohexane	20	0.42			2.2	0.94
Glycerol	20	0.34	0.52	5.0	9	1240
Glycerol	−20	0.28	1.7	11.3	18	8600

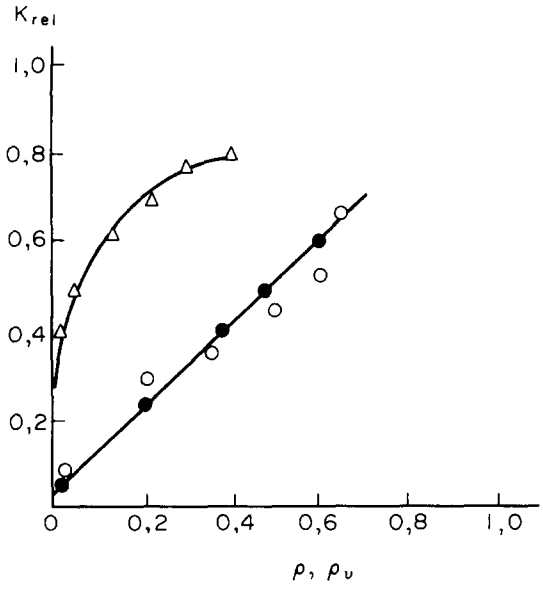

Fig. 8. Dependence of the relative parameter of ET in biantril (K_{rel}) in glycerol (●) and ethanol (○, △) on the parameters of the dynamic polarity of the solvents P' (●, ○) and P'_v (○, △) [28].

$$K=[A^+-A^-]/[A-A^S]=I(A^+-A^-)/I(A-A^S)$$
$$=k_a/(k_d+k_f+k_n) \quad (25)$$

where $A-A^S$ is biantril in the excited singlet state, I is the intensity of fluorescence, k_a is the rate constant of ET and k_d, k_f and k_n are the rate constants of recombination, radiative and non-radiative relaxation of A^+-A^- respectively. Since k_d, k_f and k_n are only slightly dependent on temperature, we expect the direct ET (k_a) to provide the main contribution to the experimental dependence of $K_{rel}=K(T)/K(300)$, where $K(T)$ and $K(300)$ are the K values at a given temperature and at 300 K.

As observed in Ref. [28], the large increase in K_{rel} at elevated temperature in glycerol ($T>240$ K) and ethanol ($T>120$ K) is accompanied by an increase in the relaxation shift of the $A-A^S$ emission spectrum. In glycerol, K_{rel} correlates with the parameters of solvent relaxation P' and P'_v which are similar for glycerol solution. For the process in ethanol, correlation between K_{rel} and the induced relaxation parameter P' takes place (Fig. 8). Therefore molecular dynamics are necessary to provide ET in the biantril molecule. This conclusion is in accord with the energy diagram of the process (Fig. 7(b)) [28] and with the data in Ref. [27a] which suggest that the motion of solvent molecules near excited biantril may be responsible for the microscopic solvation component in adiabatic ET.

6.3. Photoinduced ET in model proteins

We consider two model systems: (1) dansyl–nitroxide DAP (Section 6.1) incorporated in bovine serum albumin (BSA) in an ethylene glycol–water mixture (1:1); (2) α-chymotrypsin with the methionine-192 group modified by nitroxide as acceptor and with an intrinsic tryptophan in the excited state as donor.

The experimental temperature dependence of the rate constant of DAP fluorescence quenching (ϕ_l) [3e,3f] shows that, at a temperature below 120 K, the value of ϕ_l is not dependent on the temperature; however, with an increase in T, ϕ_l increases. The temperature at which ϕ_l increases is close to the temperature at which a change in the tryptophan phosphorescence parameters is observed, related to dynamic processes in the millisecond range [3a,4a]. Such slow dynamics cannot affect directly the excited singlet state of the donor, but allow the DAP configuration to be changed under the mechanical stress of the protein body. At $T>150$ K, a marked rise in the relaxation shift of the DAP fluorescence spectrum (λ_{max}) takes place, related to the nanosecond dynamic processes in the vicinity of the excited chromophore. At temperatures above 240 K, an increase in the rate of irreversible photo-oxidation of the nitroxide fragment (k_l) coincides with the temperature of "unfreezing" of the nitroxide fragment rotation with a correlation time $\tau_c<10^{-7}$ s.

According to the value of the relaxation shift ($\Delta\lambda_{max}$) at room temperature, the local apparent dielectric constant near the donor group of DAP in BSA is $\epsilon_{app}=12$. The value of $\epsilon_{app}=63$ in the vicinity of the nitroxide acceptor fragment was estimated by analysis of the hyperfine structure of the DAP ESR spectrum. These values were used to build up a diagram of the Gibbs energy for reversible and irreversible photochemical processes in the DAP–BSA system (Fig. 7(a)). As can be seen in Fig. 7(a), the reversible ET ($D-A\rightarrow D^+A^-$) is thermodynamically favourable over the whole temperature range. Assuming that this mechanism prevails over others (see Section 6.1), the following parameters of ET were estimated on the basis of experimental data on k_q, the local dielectric constant, the structural model of DAP and semiempirical Eqs. (11), (12) and (17) [3c]: Gibbs energy at $T=297$ K, $\Delta G_o=-1.75$ eV; Gibbs energy at $T=77$ K, $\Delta G_o=-0.25$ eV; free energy of reorganization, $E_r=0.9$ eV; resonance integral, $V=1.5\times10^{-3}$ eV; Franck–Condon factor at $T=77$ K, $FC=10^{-1}$ eV.

The photoreduction of a nitroxide acceptor covalently attached to the methionine-192 group of α-chymotrypsin by the nearest tryptophan donor in the excited singlet state has been investigated in dry powder, wet powder and aqueous solution by the ESR technique over a wide temperature region [3g]. In parallel, the microviscosity and micropolarity of the medium in the vicinity of the nitroxide and tryptophan moieties were monitored by ESR (X-band and high-resolution 2 mm band) and fluorescence spectroscopy respectively. The intermolecular dynamics of the protein globule were studied by the Mössbauer labelling technique. As can be seen from Fig. 9, the temperature dependence of the relative rate constant of the nitroxide photoreduction k_{rel} correlates with the reciprocal correlation time τ_c^{-1} of nitroxide rotation in the nanosecond range. Such dynamics appear to be necessary to stabilize the charges in the secondary redox reaction, most probably between the cation radical of the photo-oxidized

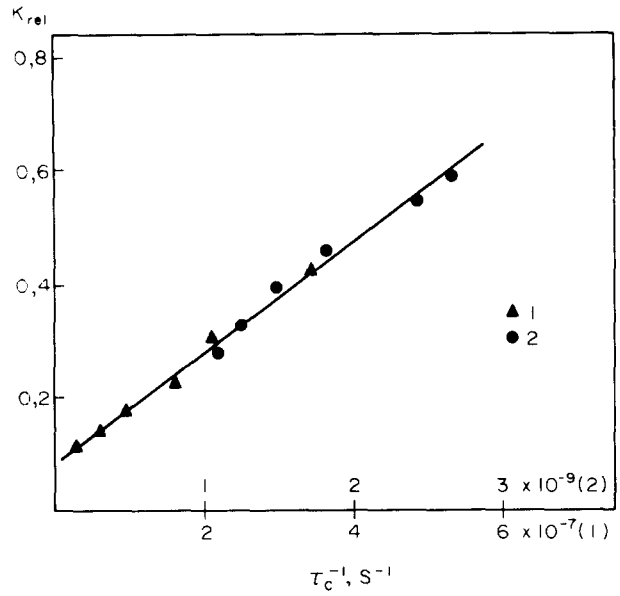

Fig. 9. Correlation plot of the relative rate constant of photoreduction of nitroxide (k_{rel}) vs. the correlation time of the nitroxide rotation (τ_c^{-1}) in spin-labelled α-chymotrypsin; 1, in a powdered state at a relative humidity $P = 0.95$; 2, in aqueous glycerol solution [3g].

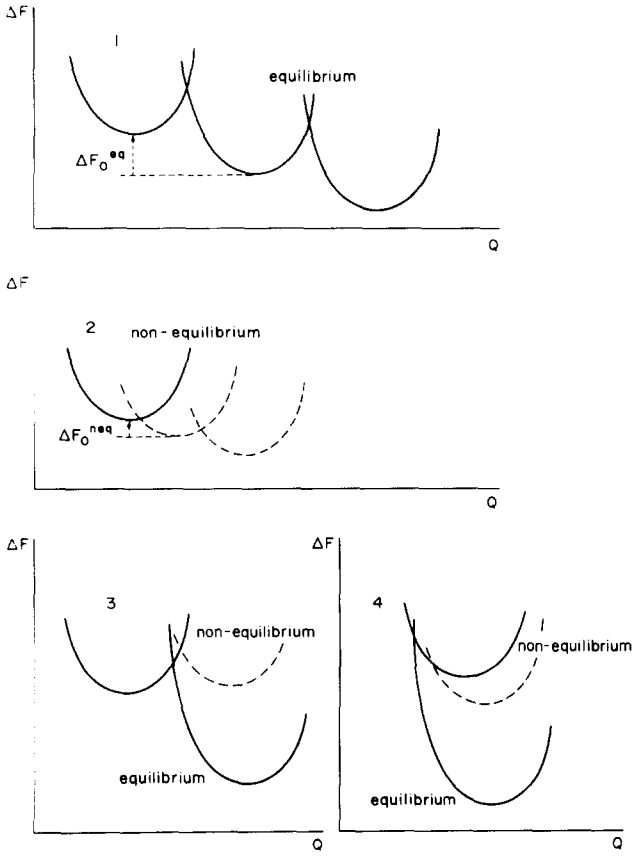

Fig. 10. Schematic representation of electronic potential energy surfaces: 1, consecutive conformational and solvational equilibrium processes with the essential change in the nuclear coordinates Q and the standard free energy ΔF_0^{eq}; 2, consecutive non-equilibrium processes with a small change in Q and ΔF_0^{neq}; 3, 4, equilibrium (full line) and non-equilibrium (broken line) processes in the normal and inverted Marcus regions respectively.

donor and the nearest group of the protein (see the energy diagram in Fig. 7(a)).

7. General discussion

An analysis of the aforementioned data allows the mechanism of the primary steps of ET in photosynthetic RCs to be discussed and the factors affecting ET in these systems to be estimated.

As shown in Section 5, the rate constants of ET from the primary donor P to an intermediate acceptor H and from H to the primary acceptor Q_A exceed the values of the correlation frequency ν_c in the experimental temperature region (Fig. 3). Such a situation indicates the formation of conformational and solvational non-equilibrium states which react before the corresponding equilibrium is attained. It can be concluded, therefore, that the elementary steps of ET in this system are not accompanied by significant shifts in the position of the medium nuclear frame nor are they governed by such shifts. The thermodynamic standard free energy for such processes (ΔF_0^{neq}) appears to be less than that involved in the case of the equilibrium dielectric stabilization of redox centres (ΔF_0^{eq}).

It can be concluded that the initial and final energy terms in the non-equilibrium case will be positioned closer to each other in space and energy compared with their positions in equilibrium (Fig. 10). Consequently, in the inverted Marcus region, the values of the reorganization energy and experimental activation energy E_a are expected to be markedly lower than in the equilibrium case. In the normal, non-inverted region, we predict a larger activation energy and a slower ET rate for non-equilibrium processes compared with equilibrium processes. The second property expected for non-equilibrium processes is the lack of dependence (Fig. 11, curve 1) or weak dependence (curve 2) of the experimental ET rate constants (for a system with close values of the resonance integral V) on ΔF_0^{eq} in both Marcus regions

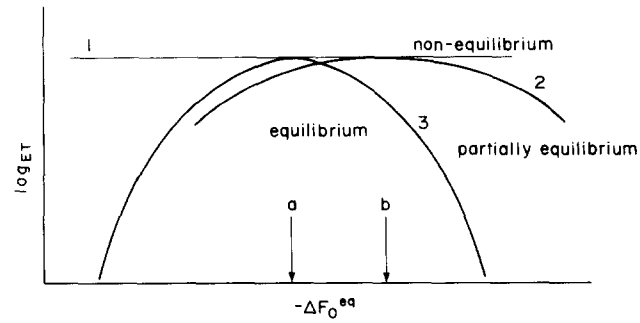

Fig. 11. Schematic representation of the dependence of the ET rate constants for processes with close values of the resonance integral on the equilibrium standard free energy (ΔF_0^{eq}): 1, conformational and solvational non-equilibrium processes with constant reorganization (E_r^{neq}) and standard free energy (ΔF_0^{neq}); 2, partial non-equilibrium processes; E_r^{neq} and ΔF_0^{neq} are slightly dependent on ΔF_0^{eq}; 3, equilibrium processes. Arrows a and b indicate conditions for the maxima $\Delta F_0^{eq} = E_r^{eq}$ and $\Delta F_0^{neq} = E_r^{neq}$ respectively.

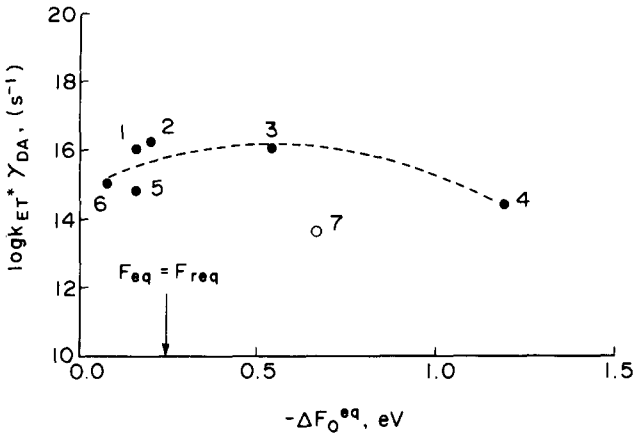

Fig. 12. Experimental values of parameter $k_{ET}\gamma_{DA}$ (k_{ET} in s^{-1}) plotted against the equilibrium standard free energy of ET (ΔF_0^{eq}). k_{ET} is the rate constant of the ET primary step in RCs from photosynthetic bacteria and plant PSI, and γ_{ET} is the attenuation parameter (see Eqs. (18) and (22)). The numbers have the same meaning as in Fig. 2. The arrow shows the position of $\Delta F_0^{eq} = E_r^{eq} = 0.26$ eV. Data on ΔF_0^{eq} and E_r^{eq} were taken from Refs. [1c–1g], [12d] and [29b].

(inverted and non-inverted), compared with that predicted by the classic Marcus expression for the equilibrium condition (curve 3) with the Franck–Condon factor [1j]

$$FC_{eq} = (2\pi E_r kT)^{-1/2} \exp\{-[(\Delta F_0^{eq} + E_r)]^2/4E_r kT\} \quad (26)$$

Eq. (18) gives

$$b = \log(\bar{k}_{ET}\gamma'_{DA}) = \log(2\pi h^{-1})|V_0|^2 FC_{eq} \quad (27)$$

where $\gamma'_{DA} = 10^{0.56 R_{DA}}$.

As can be seen in Fig. 12 for the photosynthetic RCs, the value of b depends very slightly on ΔF_{eq} in both Marcus regions. This appears to prove independently that fast primary steps of photosynthesis occur in non-equilibrium conditions and all the ETs have similar values of the Franck–Condon factor. A deviation of the data from the uniform dependence on ET from Q_A^- to P^+ is plausibly accounted for by the equilibrium character of the process with a slow rate of ET ($k_{ET} = 2 \times 10^4$ s^{-1}) relative to the rate of protein dynamic relaxation.

According to Refs. [1a–1d] and [29], a reaction channel of ET may involve final vibrationally excited states and have an activation energy which may be lower than that of the vibrationally unexcited channel. In such a case, the inverted region is also characterized by a rate independent of the temperature and the standard free energy. Nevertheless, in the case of a non-equilibrium mechanism, such an independence is also expected in the non-inverted region. At present, it is difficult to estimate the quantitative contribution of the two mechanisms (vibrational excitation and non-equilibrium condition) to the given ET process in the inverted region.

According to Eq. (17), at an edge–edge distance between donor and acceptor centres of $R_{DA} > 7$–8 Å in non-conducting media, the value of the resonance integral $V < 2.6 \times 10^{-2}$ eV. Thus the ET process is expected to be non-adiabatic. Therefore all steps of ET from the primary donor P to the primary acceptor Q_A proceed non-adiabatically and Eq. (18) with the coefficient $\beta_{DA} = 1.3$ Å can be used to estimate the average value of the Franck–Condon factor. An approximate estimate of FC according to the data presented in Fig. 2 gives $FC = 0.15$–0.2 eV^{-1}.

ET from the primary acceptor Q_A to the secondary acceptor Q_B with the rate constant $k_{QAQB} = 1.5 \times 10^4$ s^{-1} can be considered to be adiabatic and the rate of the process is not expected to be dependent on the value of the resonance integral (Section 4). It is known [1e,12a,12b,12d] that substitution of Fe^{2+} in the RC of purple bacteria by other divalent metals, either paramagnetic or diamagnetic, completely restores the kinetics to the values observed in native RC. The adiabatic character of ET accounts for this apparently puzzling effect. At physiological temperatures, the correlation time of the intramolecular dynamics of the RC is found to be in the nanosecond range and k_{QAQB} is of the order of microseconds. It follows that ET occurs between the donor and acceptor centres in the equilibrium state.

A slight dependence of the rate constant of ET on the temperature and the momentary and static polarity in the Marcus inverted region was also observed in model DAPs in liquids [2j,3b,3c,5k]. In the aforementioned DAP in glycerol solution (Section 6.1), the process of fluorescence quenching, most probably caused by the reversible ET mechanism, is found to be 2–6 times faster than the spectral relaxation process.

In all the systems mentioned in this section, ET is energetically allowed in non-equilibrium conditions. In other cases (ET in excited biantril, irreversible reduction of the nitroxide acceptor in DAP in liquids and BSA and in α-chymotrypsin (Section 6) and the $Q_A^- \rightarrow Q_B$ transition in RC (Section 5)), it was found that the reaction coordinate is the solvent coordinate and that the dielectric relaxation in the nanosecond temporal region is favourable for a given ET energetic profile (Fig. 7).

Other effects were observed in DAPs in proteins: a decrease in the rate constant of the $Q_A^- \rightarrow P^+$ recombination and an increase in the ET rate in DAP incorporated in BSA with a "defreezing" of the medium modes in the millisecond range (Section 6.3). These effects can be caused by a change in the distance and mutual orientation of the donor and acceptor centres with a rise in temperature.

8. Conclusions

The dependence of the rate constants of the primary steps of ET in the RCs of photosynthetic bacteria and PSI on the distance between the donor and acceptor groups was found to be close to the corresponding dependence of the attenuation parameter of SE (γ_{SE}) through a "non-conducting" organic medium on the distance between the exchangeable centres. This establishes SE as an idealized model of ET. On the basis of this assumption, the attenuation parameter (γ_X) for spin superexchange through individual chemical groups in biradicals and complexes of transition metals with paramagnetic

ligands can be used for the estimation of the values of the resonance integral (V), which is an essential parameter of ET theory. Values of γ_X for groups of importance in ET in biological and model systems have been calculated on the basis of the experimental exchange integrals (J) and have been tabulated.

The calculated values of γ_{SE} and γ_X were used to estimate the resonance integrals and Franck–Condon factors (FC) in ET primary steps in the RCs. The value of FC = 0.15–0.2 eV was found to be similar for all steps. For ET from the primary quinone acceptor Q_A to the secondary quinone acceptor Q_B, the estimated value of V exceeds the threshold for adiabatic processes and the process can be considered to be adiabatic.

Estimating the resonance integral V allows the relationship between kinetics and thermodynamics to be analysed, including the predictions of Marcus theory, for systems with different V.

Parallel investigations of the rates of ET and molecular dynamics, monitored by physical labelling techniques over a wide range of temperature (77–300 K) and correlation time ($\tau_c = 10^{-2}$–10^{-10} s), in photosynthetic RCs and model DAPs in simple liquids and proteins allow the effects of dynamics on ET to be studied. The general trends are as follows:

(1) if ET is faster, due to vibrational modes, than the dipole relaxation of the surrounding molecules, the ET rate constants depend only slightly on the medium relaxation correlation time, micropolarity, local viscosity and temperature; the k_{ET} values are expected to depend only slightly on the equilibrium standard free energy (ΔF_0^{eq}) in inverted and non-inverted Marcus regions (ET in RC and in DAP in liquids);

(2) relatively slow millisecond dynamics can allow the distance and mutual orientation of donor–acceptor groups to be changed, which leads to a change in the ET rate with an increase in temperature ($Q_A^- \rightarrow P^+$ recombination, DAP in BSA);

(3) nanosecond dynamics are necessary to provide favourable thermodynamics and low reorganization free energy by the stabilization of charges ($Q_A^- \rightarrow Q_B$ transition, photoreduction of nitroxides);

(4) very fast adiabatic ET in biantril is limited by the induced dipole relaxation in the vicinity of the solute.

Acknowledgements

The author wishes to thank Professors Shlomo Efrima and David Gil for valuable discussions and critical comments, Dr. Elena Rubtsova for assistance in the compilation of Table 1 and Dr. Alexander Shames for generous help in the preparation of the manuscript.

References

[1] (a) J. Jortner, *J. Chem. Phys., 64* (1976) 4860; (b) I. Rips, J. Klafter and J. Jortner, *J. Phys. Chem., 94* (1990) 8557; (c) M. Bixon and J. Jortner, *J. Phys. Chem., 95* (1991) 1941; (d) J. Jortner and M. Bixon, *J. Photochem. Photobiol. A: Chem., 82* (1994) 5; (e) J.R. Norris, *Israel J. Chem., 32* (1992) 412; (f) M. Bixon, *Israel J. Chem., 32* (1992) 422; (g) R. Nechushtai, *Israel J. Chem., 32* (1992) 441; (h) D. DeVault, *J. Q. Rev. Biophys., 13* (1990) 387; (i) J.J. Hopfield, *Proc. Natl. Acad. Sci. USA, 71* (1974) 3640; (j) H.B. Gray and J.R. Winkler, *Pure Appl. Chem., 64* (1992) 1257; (k) R. Marcus and N. Sutin, *Biochim. Biophys. Acta, 811* (1985) 265; (l) S.E. Peterson-Kennedy, J.L. McGourty and B.H. Hoffman, *J. Am. Chem. Soc., 104* (1984) 5010; (m) A. Warshal and W.W. Parson, *Annu. Rev. Phys. Chem., 42* (1991) 279.

[2] (a) G.L. McLendon, *Acc. Chem. Res., 21* (1988) 160; (b) H. Lebanon and K. Mobius, *Israel J. Chem., 32* (1992) 457; (c) J.L. Sessler, *Israel J. Chem., 32* (1992) 449; (d) M.R. Wasielewski, *Chem. Rev., 92* (1992) 435; (e) J.S. Connolly and J.R. Bolton, in M.A. Fox and Channon (eds.), *Photoinduced Electron Transfer*, Part D, Elsevier, Amsterdam, 1988; (f) E.M. Kosover and D. Huppert, *Annu. Rev. Phys. Chem., 37* (1986) 127; (g) A.I. Hoff, H. Lebanon and D. Stehlik, *Israel J. Chem., 32* (1992) 399; (h) R.A. Marcus, in T. Frangsmyr (ed.), *Lex Prix Nobel*, Almquist and Wiksell, Stockholm, Sweden, 1993, p. 63; (i) J.D. Simon, *Acc. Chem. Res., 21* (1988) 128; (j) J.L. Sessler, *Israel J. Chem., 32* (1992) 449; (k) G. Feher, *Israel J. Chem., 32* (1992) 431.

[3] (a) G.I. Likhtenshtein, *Chemical Physics of Metalloenzyme Catalysis*, Springer Verlag, Heidelberg, 1988; (b) S.M. Bystrjak, G.I. Likhtenshtein, A.I. Kotelnikov and K. Hideg, *J. Phys. Chem. (Moscow), 61* (1986) 2769; (c) G.I. Likhtenshtein, S.M. Bystrak and A.I. Kotelnikov, *Chem. Phys. (Moscow), 5* (1990) 69; (d) S.M. Bystrjak, G.I. Likhtenshtein and A.I. Kotelnikov, *Chem. Phys. (Moscow), 11* (1992) 37; (e) E.T. Rubtsova, V.R. Vogel, D.V. Khudjakov, A.I. Kotelnikov and G.I. Likhtenshtein, *Biophysics, 38* (1993) 211; (f) V.R. Vogel, E.T. Rubtsova, G.I. Likhtenshtein and K. Hideg, *J. Photochem. Photobiol. A: Chem., 83* (1994) 229; (g) O.V. Belonogova, G.I. Likhtenshtein and V.I. Krinichny, *Eur. J. Biophys.*, submitted for publication.

[4] (a) G.I. Likhtenshtein, *Biophysical Labeling Method in Molecular Biology*, Cambridge University Press, Cambridge, New York, 1993; (b) A.I. Berg, A.F. Kononenko, P.P. Noks, I.N. Khrimova, E.N. Frolov, A.B. Rubin and G.I. Likhtenshtein, *Mol. Biol. (Moscow), 13* (1979) 469; (c) A.I. Berg, P.P. Noks, A.A. Kononenko, E.N. Frolov, A.B. Rubin, G.I. Likhtenshtein, V.I. Goldansky, F. Parak, M. Bukl and R.L Mössbauer, *Mol. Biol. (Moscow), 13* (1979) 81; (d) V.I. Goldansky, A.F. Kononenko, A.B. Rubin, E.N. Frolov and D.S. Chernavsky, *Dokl. Akad. Nauk SSSR, 257* (1981) 491; (e) G.I. Likhtenshtein and A.I. Kotelnikov, *Mol. Biol. (Moscow), 17* (1983) 505; (f) G.I. Likhtenshtein, *Biofizika, 30* (1985) 27.

[5] (a) L.D. Zusman, *Chem. Phys., 49* (1980) 295; (b) I.V. Alexandrov, *Chem. Phys., 51* (1980) 445; (c) I. Rips and J. Jortner, *J. Chem. Phys., 88* (1980) 818; (d) A.I. Burshtein and A.A. Jarikov, *Chem. Phys., 152* (1991) 23; (e) J.T. Hynes, *J. Phys. Chem., 90* (1986) 3701; (f) W. Nadler and R. Marcus, *Chem. Phys. Lett., 144* (1988) 24; (g) J. Wang and P. Wolynes, *Chem. Phys., 180* (1994) 141; (h) T. Fonesca, *J. Chem. Phys., 91* (1989) 2869; (i) H. Sumi and R. Marcus, *J. Chem. Phys., 84* (1986) 4894; (j) M.P. Maroncelli, J. MacInnes and G.R. Fleming, *Science, 243* (1989) 1634; (k) E. Åkesson, G.C. Walker and P.F. Barbara, *J. Chem. Phys., 95* (1991) 4188; (l) R.J. Harrisson, B. Pearce, G.S. Beddard, J.A. Cowan and J.K.M. Sanders, *Chem. Phys. 116* (1987) 429; (m) M.D. Todd, A. Nitzan, M.A. Ratner and J.T. Hupp, *J. Photochem. Photobiol. A: Chem., 82* (1994) 87; (n) D.C. Mauzerall and J.S. Lindsay, *J. Am. Chem. Soc., 112* (1990) 957.

[6] (a) V.G. Levich and R.R. Dogonadze, *Dokl. Akad. Nauk. SSSR, 124* (1959); (b) R.R. Dogonadze, A. Kuznetsov and J. Ulstrup, *J. Theor. Biol., 69* (1977) 239.

[7] L.A.Q. Blumenfeld, *Rev. Biophys., 11* (1978) 251.

[8] (a) G.I. Likhtenshtein, T.V. Troshkina, Ju.D. Akhmedov and V.F. Shuvalov, *Mol. Biol. (Moscow), 3* (1969) 413; (b) Ju.D. Akhmedov and G.I. Likhtenshtein, *Mol. Biol. (Moscow), 4* (1970) 551; (c) G.I.

Likhtenshtein, *Stud. Biophys., 33* (1972) 185; (d) E.N. Frolov, A.P. Mokrushin, G.I. Likhtenshtein, V.A. Trukhtanov and V.I. Goldanskii, *Dokl. Akad. Nauk SSSR, 12* (1972) 165; (e) V.P. Timofeev, O.L. Polyanovskii, M.V. Volkenshtein and G.I. Likhtenshtein, *Biochim. Biophys. Acta, 220* (1970) 357; (f) E.N. Frolov, G.I. Likhtenshtein, O.V. Belonogova and Ju.I. Khurgin, *Bull. Acad. Sci. USSR (Chem.), 7* (1973) 135; (g) E.N. Frolov, G.I. Likhtenshtein and N.V. Kharakhonicheva, *Mol. Biol. (Moscow), 8* (1974) 824; (h) G.I. Likhtenshtein, in A. Alfsen (ed.), *L'Eau les Systems Biologique*, Editions CNRS, Paris, 1976; (i) G.I. Likhtenshtein, *Spin Labeling Methods in Molecular Biology*, Wiley Interscience, New York, 1976; (j) G.I. Likhtenshtein, *Biophysics (Moscow), 30* (1985); (k) G.I. Likhtenshtein, *Stud. Biophys., 111* (1986) 89.

[9] G.I. Likhtenshtein, V.R. Bogatirenko and A.V. Kulikov, *Appl. Magn. Reson., 4* (1993) 513.

[10] (a) A.I. Kotelnikov, V.R. Fogel, G.I. Likhtenshtein, E.I. Shljapnikova and E.B. Postnikova, *Mol. Biol. (Moscow), 15* (1981) 281; (b) K.I. Zamaraev, Y.N. Molin and K.M. Salikhov, *Spin Exchange. Theory and Physico-Chemical Application*, Springer Verlag, Heidelberg, 1981; (c) G.I. Likhtenshtein, A.V. Kulikov, A.I. Kotelnilov and V.R. Bogatyrenko, *Photochem. Photobiol., 3* (1982) 337; (d) K.M. More, G.R. Eaton, S.S. Eaton, O.H. Hankovsky and K. Hideg, *Inorg. Chem., 28* (1989) 1734; (e) G.R. Eaton and S.S. Eaton, *Acc. Chem. Res., 21* (1988) 107; (f) J.K. More, K.M. More, G.R. Eaton and S.S. Eaton, *Pure Appl. Chem., 62* (1990) 241; (g) V.N. Parmon, A.I. Kokorin and G.M. Zhidomirov, *Stable Biradicals*, Nauka, Moskow, 1980; (h) G.L. Closs, M.D. Johnson, J.R. Miller and P. Piotrowiak, *J. Am. Chem. Soc., 111* (1989) 3751; (i) G.I. Likhtenshtein, *Pure Appl. Chem., 62* (1990) 281; (j) G.I. Likhtenshtein, *J. Mol. Catal., 48* (1988) 129; (k) A.I. Kotelnikov, *Biofizika, 38* (1993) 228.

[11] (a) A.L. Buchachenko and A.M. Wasserman, *Stable Radicals*, Khimiya, Moscow, 1973; (b) G.R. Luckhurst, Biradicals as spin probes, in L. Berliner (ed.), *Spin Labeling. Theory and Applications*, Academic Press, New York, 1976; (c) F.A. Neugebauer and R. Bernhard, *Chem. Ber., 110* (1977) 2254; (d) A.I. Kokorin, B.N. Parmon, V.I. Suskina, Yu.A. Ivanov, E.G. Rozanzev and K.I. Zamaraev, *J. Phys. Chem. (Moscow), 48* (1974) 953; (e) S.N. Glarum and J.H. Marshal, *J. Chem. Phys., 47* (1967) 1374; (f) S. Ohnishi, J.R. Cyr and H. Fukushima, *Bull. Chem. Soc. Jpn., 43* (1970) 673; (g) A. Nakajama, H. Ohya-Nishigushi and Y. Deduchi, *Bull. Chem. Soc. Jpn., 45* (1972) 713; (h) A. Rassat, *Pure Appl. Chem., 62* (1990) 213.

[12] (a) J. Deisenhofer and H. Michel, *EMBO J., 8* (1989) 2149; (b) G. Feher, J.P. Allen, M.Y. Ocamura and D.C. Rees, *Nature, 339* (1989) 111; (c) N. Krauss, W. Hinrichs, I. Witt, P. Fromme, W. Pritzkov, Z. Dautr, C. Betzel, K.S. Wilson, H.T. Witt and W. Seanger, *Nature, 361* (1992) 323; (d) G. Feher, *Israel J. Chem., 32* (1992) 431; (e) J.P. Allen, G. Feher, T.O. Yeates, H. Komiya and D.C. Rees, *Proc. Natl. Acad. Sci. USA, 84* (1987) 6162.

[13] (a) C. Kirmaier, D. Gaul, R. de Bey, D. Holten and C.C. Shenck, *Science, 251* (1991) 922; (b) M.H. Vos, J.C. Lambry, S.J. Robles, D.C. Youvan, J. Breton and J.L. Martin, *Proc. Natl. Acad. Sci. USA, 89* (1991) 613; (c) C.K. Chan, T.J. DiMagno, L.X.Q. Chen, J.R. Norris and G.R. Fleming, *Proc. Natl. Acad. Sci. USA, 88* (1991) 11 202; (d) C. Kirmaier, D. Holton and W.W. Parson, *Biochim. Biophys. Acta, 810* (1985) 49; (e) M.R. Gunner, *Curr. Top. Bioenergetics, 16* (1991) 319; (f) A. Vermeglio and R.K. Clayton, *Biochim. Biophys. Acta, 461* (1977) 159; (g) J.D. McElroy, G. Feher and D.C. Mauzerall, *Biochim. Biophys. Acta, 172* (1969) 180; (h) C.C. Moser, J.M. Keske, K. Warncke, R.S. Farid and R.S. Dutton, *Nature, 335* (1992) 796.

[14] D.L. Dexter, *J. Chem. Phys., 21* (1953) 836.

[15] (a) S. Larsson, *Faraday Discuss. Chem. Soc., 74* (1982); (b) M.D. Newton, *Faraday Discuss. Chem. Soc., 74* (1982) 110; (c) S. Larsson and M. Braga, *J. Photochem. Photobiol. A: Chem., 82* (1994) 61; (d) C. Liang and M.D. Newton, *J. Phys. Chem., 96* (1992) 2855; (e) J.R. Reimers and N.S. Hush, *J. Photochem. Photobiol. A: Chem., 82* (1994) 31; (f) A. Cheong, A.E. Roitberg, V. Mujica and M.A. Ratner, *J. Photochem. Photobiol. A: Chem., 82* (1994) 81; (g) J. Tang and J.R. Norris, *Chem. Phys., 175* (1993) 337–342; (h) D.N. Beratan, J.N. Betts and J.N. Onuchic, *J. Phys. Chem., 96* (1992) 2852.

[16] A.R. Forrester and S.P. Hepburn, *J. Chem. Soc., 6* (1971) 701.

[17] A.B. Shapiro, G.A. Novozhilova and E.G. Rozantzev, *Bull. Acad. Sci. USSR (Chemistry),* (1976) 452.

[18] J.J. Owen, *Appl. Phys. Suppl., 33* (1962) 355.

[19] R.P. Shibaeva, *J. Struct. Chem. (Moscow), 16* (1975) 330.

[20] W. Plachy and D. Kivelson, *J. Chem. Phys., 47* (1967) 3312.

[21] (a) L. Berliner (ed.), *Spin Labeling. Theory and Applications*, Vols. 1 and 2, Academic Press, New York, 1976 and 1979; (b) L. Berliner and J. Reuben (eds.), *Spin Labeling. Theory and Applications*, Plenum, New York, 1989.

[22] (a) J.R. Lakowicz, *Principles of Fluorescence Spectroscopy*, Plenum, New York, 1983; (b) J.R. Lakowicz (ed.), *Topics of Fluorescence Spectroscopy*, Plenum, New York, 1991; (c) Yu.T. Mazurenko and N.G. Bakhsheev, *Opt. Spektrosk., 28* (1990) 905.

[23] S.M. Bystryak, G.I. Likhtenshtein and A.I. Kotelnikov, *J. Appl. Spectrosc. (Minsk), 52* (1990) 392.

[24] (a) S.M. Bystryak, G.I. Likhtenshtein and A.I. Kotelnikov, *Chem. Phys. (Moscow), 9* (1990) 697; (b) G.I. Likhtenshtein, A.I. Kotelnikov, V.R. Vogel and G.B. Postnikova, *J. Appl. Spectrosc. (Minsk), 40* (1984) 564.

[25] D.M. Gakamsky, G.I. Likhtenshtein, R. Shuker, E. Haas, A. Goldin and K. Hideg, *J. Fluorescence*, submitted for publication.

[26] (a) J. Green and L.A. Singer, *J. Chem. Phys., 58* (1977) 2659; (b) V.A. Kuzmin and A.S. Tatikilov, *Chem. Phys. Lett., 51* (1977); (c) S.A. Green, D.J. Simpson, G. Johnson, P.S. Ho and N.V. Blough, *J. Am. Chem. Soc., 112* (1990) 7337.

[27] (a) T.A. Kang, W. Jarzeba, P.F. Barbara and T. Fonesca, *Chem. Phys., 149* (1990) 81; (b) M. Mas, J. Naibar and J. Witz, *J. Photochem. Photobiol. A: Chem., 88* (1995) 93.

[28] S.M. Bystriak, G.I. Likhtenshtein and A.V. Kotelnikov, *Chem. Phys. (Moscow), 11* (1992) 374.

[29] (a) S. Efrima and M. Bixon, *Chem. Phys. Lett., 25* (1974) 34; (b) M. Bixon, J. Jortner and M.E. Michel-Beyerle, *Biochim. Biophys. Acta, 1056* (1991) 301.

[30] H.M. McConnel, *J. Chem. Phys., 33* (1960) 115.